



International Journal of Recent Development in Engineering and Technology
Website: www.ijrdet.com (ISSN 2347-6435(Online) Volume 7, Issue 6, June 2018)

Dielectric Properties of Transparent CdS Nanofibers Synthesized via dc-Sputtering Technique

Pradip Kumar Ghosh

Department of Physics, Abhedananda Mahavidyalaya, Sainthia, Birbhum, W.B, India

Abstract— CdS nanofibers have been prepared by direct current-sputtering technique without using any catalyst or matrix. X-ray diffraction patterns and selected area electron diffraction patterns confirmed the cubic CdS phase formation in the thin films although; the initial target material was hexagonal CdS powder. TEM micrographs have confirmed the nanofiber formation with diameters in the range 2 - 4.3 nm and length a few microns. XRD patterns showed the crystal size increased with the increase of deposition time. UV-Vis spectra of the films have showed nearly 90 % transparency in the visible range and bandgap is higher compared to that of the bulk material. The direct bandgap increased from 3.06 eV to 3.56 eV with decrease of deposition time 20 to 7 min. The crystallite sizes have also been determined from the shift of direct bandgap with that of bulk CdS and they lie in the range 2.82 - 3.65 nm. The dielectric constant for thin films of CdS nanofibers have been measured under vacuum by using an L-C-R meter and the value of it lies in the range 55 to 73 at higher frequencies.

Keywords— CdS nanofibres; dc-sputtering; nanostructural; optical, dielectric properties.

I. INTRODUCTION

Nanocrystalline semiconductors, which can be grown efficiently in different form such as nanoparticles, nanorods, nanobelts, nanowire etc, have attracted much attention due to their novel properties and promising applications. Various nanodevices including nanologic circuits, nanolasers, nanosensors, nanothermometers [1], etc. have been assembled using one-dimensional nanoscale materials. Transparent quantum dots and quantum wires of II-VI sulfide semiconductors such as CdS and ZnS have gained renewed interest due to their enhanced luminescence property and size dependent optical properties. Depending on the sizes of the particles, the nanoscale semiconductors show interesting properties [2-5], and great efforts have been imposed upon controlling their sizes. Starting from the zero-dimensional nanoparticles, various structures such as nanowires, nanorods, nanotubes and nanobelts have been produced from different materials in different routes.

It is well known that CdS is a II-VI semiconductor having a direct bandgap 2.42 eV.

It has many commercial applications such as in photoelectric devices and in solar cells. Previously, different properties of CdS thin films studied by different groups [6-7] deposited by various routes such as pulsed laser deposition (PLD), vacuum evaporation, rf sputtering, chemical bath deposition (CBD) etc. Dielectric properties of CdS was also studied by different groups [8-13]. But the report on CdS nanostructure formation via dc-sputtering is scanty. In this letter we have reported the synthesis of CdS nanofibres by dc-sputtering without using any catalyst, and studied their structural and optical properties with varying deposition time. Sputtering is a well-known technique for the deposition of thin films. For polycrystalline film synthesis by sputtering, in general the sputtering pressure is kept low $< 10^{-1}$ mbar. This would allow the adatoms on the substrate enough mobility for growing bigger crystallites. In this work we have studied the dielectric properties of CdS nanofibres prepared at high pressure dc-sputtering technique.

II. EXPERIMENTAL

Target of cadmium sulfide (CdS) was fabricated by taking a suitable aluminium holder (5 cm dia.) and compacting the CdS polycrystalline powder (Aldrich, purity 99.99%) by applying suitable hydrostatic pressure (~ 100 kg / cm²). The fabricated CdS target was placed in the dc-sputtering chamber for the deposition of nanocrystalline thin films on various substrates.

The films were synthesized at room temperature and the substrates used were glass and Si. The glass substrates were cleaned at first by a mild soap solution, then in boiling water and in an ultrasonic cleaner and finally degreased in alcohol vapor. For Si substrates, to remove the surface oxide layer, they were etched in HF ($\sim 20\%$) for 5 minutes and finally cleaned in an ultrasonic cleaner. The chamber was evacuated by conventional rotary and diffusion pump combination to a base pressure of 10^{-6} mbar. Before starting the actual deposition the target was pre-sputtered and the substrates were covered by a movable shutter. The working pressure of the evacuated chamber was maintained at ~ 0.5 mbar by sending argon gas during deposition of the film.

Sputtering was performed at 1.7 kV and corresponding current density was 3.2 mA/cm^2 . The distance of the target and substrate was $\sim 1.6 \text{ cm}$. For TEM measurement the films were scratched out carefully by a sharp knife edge from some portion of the glass substrates. These particles were dispersed in ethanol by ultrasonication and then a few drop of this solution, was placed on carbon coated copper grid and it was allowed to dry out. For different deposition time different carbon coated copper grids were used and the materials on carbon coated copper grid were utilized to measure the TEM image.

The deposited films were characterized by studying mainly structural and optical properties. UV-Vis transmittance measurement was performed by using a spectrophotometer (Hitachi U3400). For structural studies an X-ray diffractometer (Bruker D8 Advance) was used. XRD pattern was measured in the 2θ range $20 - 70^\circ$ using $\text{Cu K}\alpha$ radiation ($\lambda = 0.15406 \text{ nm}$). For TEM measurement a transmission electron microscope (Hitachi 600) was used.

The dielectric properties of the films were also studied with varying frequency by using an L-C-R meter (HP - 4284 A) at room temperature under vacuum ($\sim 10^{-3} \text{ mbar}$).

III. RESULTS AND DISCUSSION

A. Nanostructural and X-Ray Diffraction studies

The transmission electron micrographs of the nanocrystalline CdS thin films are as shown in Fig.1 (A), (B), (C) and Inset of each figure shows the corresponding selected area electron diffraction (SAED) patterns. Presence of CdS nanofibres is clearly visible in TEM micrographs and the corresponding diffraction pattern of the film consists of central halo and concentric rings. From the diameter of the rings, we calculated the inter-planer spacing (d) values, which corresponded to reflection from (111) and (220) planes of cubic CdS. The average diameter of the nanofibres lie within the range 2 nm to 4.3 nm and the length is of the order of micron. It is also clear from the TEM micrographs that the diameters of the nanofibres increase with the increase of deposition time.

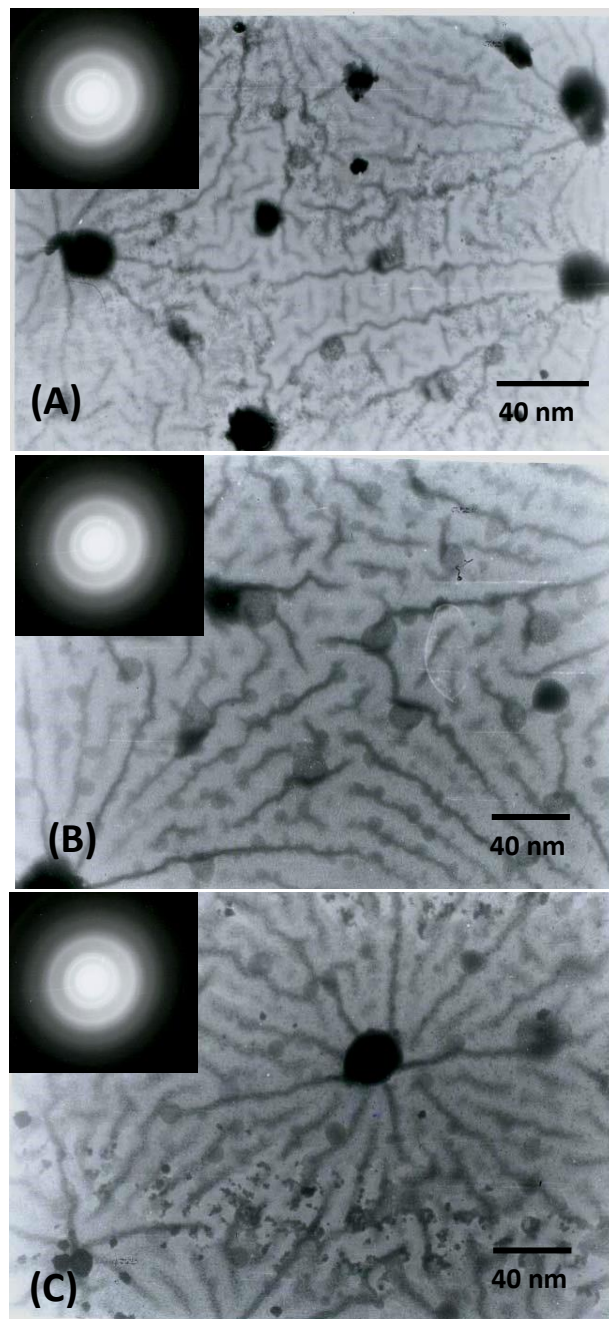


Fig.1. Transmission electron micrographs (A), (B) and (C) for different deposition time and Inset: SAED pattern of each the thin film deposited on carbon coated copper grid.

Table I:
 COMPARISON OF INTERPLANER SPACING (D) VALUES OBTAINED FROM
 XRD, TEM, JCPDS DATA CARD.

d_{XRD} (Å)	d_{TEM} (Å)	d_{JCPDS} (Å)	hkl
3.36	3.36	3.36	1 11
2.03	2.05	2.05	220
1.76	--	1.75	311

X-ray diffraction patterns of CdS powder (target material) and thin films were studied. For target material, the several peaks of hexagonal phase of CdS powder with $a = b = 4.136 \text{ \AA}$, $c = 6.713 \text{ \AA}$, have been obtained due to reflections from (100), (002), (101), (102), (110), (103), (112), (203) and (211) planes of CdS as shown in Fig.2 (A). For thin films, only the reflection from (111), (220) and (311) planes of cubic CdS ($a_0 = 5.818 \text{ \AA} = b_0 = c_0$) for deposition time 10 min., 15 min., 20 min. and 25 min. were obtained, as shown in (a), (b), (c) and (d) respectively in Fig.2 (B). Also the peaks are broadened due to the nanocrystallinity of the films. Here it should also be noted that for deposition time below 10 min., no peak in XRD was obtained. This might be due to the fact that for very small deposition time, the films are amorphous in nature. The information on strain (ϵ) and the crystallite size (L) of CdS thin films have been obtained from the following Debye-Scherrer relations:

$$L = \lambda / \beta \cos\theta, \text{ and } \epsilon = \beta / 4\tan\theta \quad (1)$$

where β is the Full-Widths-at-Half-Maximum (FWHM) of the diffraction peaks. The strain values lie in the range 7.2×10^{-2} to 1.9×10^{-2} and the crystallite sizes lie within the range 2.3 nm to 4.6 nm. The crystallite strain decreases with the increase of crystallite size. The interplaner spacing (d) corresponding to XRD peaks, TEM measurement and JCPDS Card [14] have been compared as shown in Table I.

B. Optical absorption and optical band gap:

Fig. 3 shows the transmission spectra of the nanocrystalline CdS films deposited on glass substrates. The band gap of the films $E_{g(\text{film})}$ was determined from the transmission vs. wavelength traces (as shown in Fig. 3) recorded in the range 300 - 900 nm prepared in different deposition time. These show ~ 85% transmittance in the wavelength range of 550 nm to 900 nm. The fundamental absorption, which corresponds to electron excitation from the valance band to conduction band, can be used to determine the nature and value of the optical band gap.

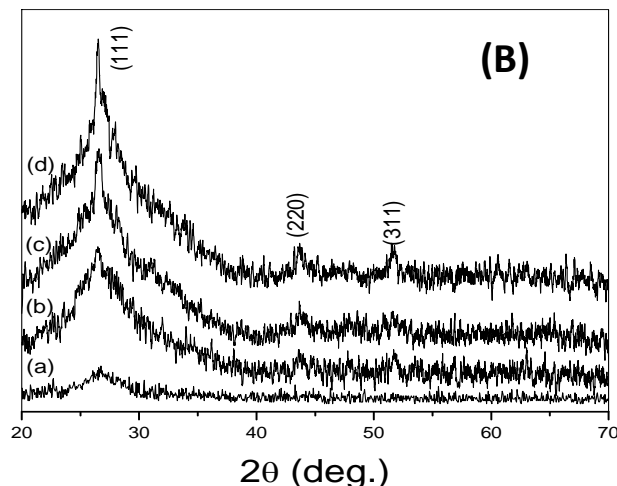
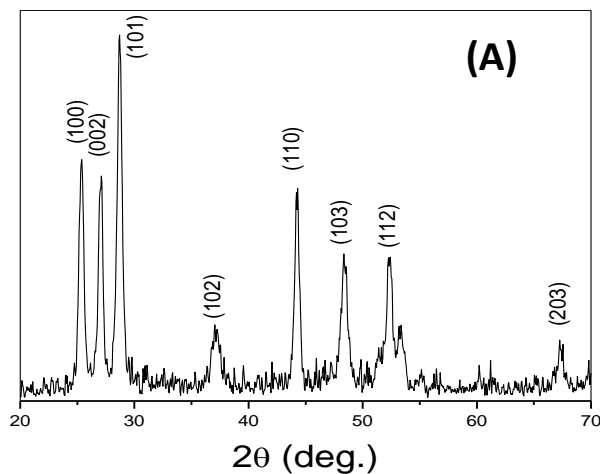


Fig.2. (A). XRD spectrum of the CdS target material and (B). XRD patterns of a nanocrystalline CdS thin films deposited on glass substrates for deposition time (a) 10 min., (b) 15 min., (c) 20 min. and (d) 25 min.

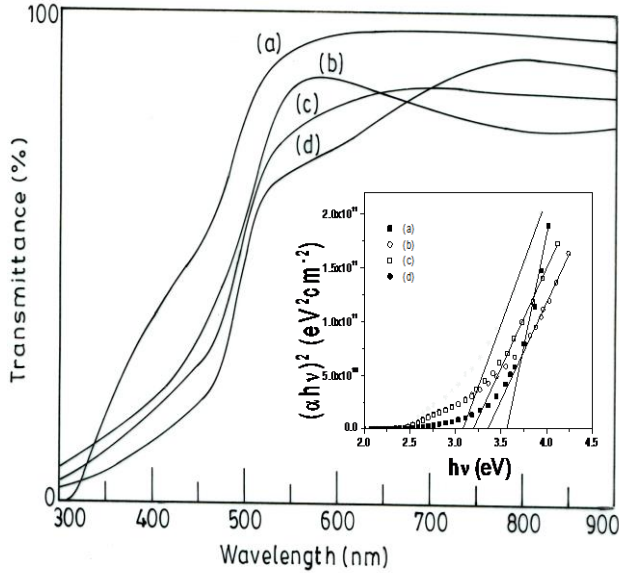


Fig.3. Transmittance spectra of representative nanocrystalline CdS thin films on glass substrates (a) t = 7 min.; (b) t = 10 min.; (c) t = 15 min. and (d) t = 20 min. Inset: Plot to determine the direct band gap of nanocrystalline CdS thin films for different deposition time.

The relation between the absorption coefficients (α) and the incident photon energy ($h\nu$) can be written as [15],

$$(\alpha h\nu)^{1/n} = A(h\nu - E_g) \quad (2)$$

where A is a constant and E_g is the band gap of the material and exponent n depends on the type of transition. For direct allowed $n = 1/2$, indirect allowed transition, $n = 2$, and for direct forbidden, $n = 3/2$. To determine the possible transitions, $(\alpha h\nu)^{1/n}$ vs. $h\nu$ were plotted and corresponding band gaps were obtained by extrapolating the straight portion of the graphs on $h\nu$ axes at $\alpha = 0$. The direct and indirect band gaps (as shown in Table II) determined from $(\alpha h\nu)^2$ vs. $h\nu$ plots (as shown in inset of Fig.3) and $(\alpha h\nu)^{1/2}$ vs. $h\nu$ plots (not shown here) for different deposition times respectively. The direct band gap values of the films lies in the range 3.06 eV to 3.56 eV are higher than that of bulk value of CdS (2.42 eV) because of quantum confinement of CdS nanocrystals and the indirect band gap lies in the range 1.3 eV to 2 eV which are also higher.

TABLE II:
 COMPARISON OF DEPOSITION TIME, DIRECT BANDGAP, INDIRECT BANDGAP AND CRYSTALLITE SIZE FROM SHIFT OF DIRECT BANDGAP.

Name of the sample	Deposition time (min.)	Direct band gap (eV)	Indirect band gap (eV)	Crystallite size (nm)
(a)	7	3.56	2.0	2.82
(b)	10	3.39	1.66	3.23
(c)	15	3.20	1.37	3.41
(d)	20	3.06	1.3	3.65

The properties of nanocrystalline materials are changed from their corresponding bulk properties due to the crystallite size become comparable to the Bohr excitonic radius (r_B).

$$r_B = h^2 \varepsilon [1 / m_e^* + 1 / m_h^*] / \pi e^2 \quad (3)$$

where ε is the permittivity of the sample, $m_e^* = 0.21m_0$ and $m_h^* = 0.80m_0$ are the effective mass of electron and hole in CdS respectively, where m_0 is the mass of a free electron. From the above relation the Bohr radius of CdS has been calculated to be 2.8 nm. The values of the crystallite size of the nanofibers, as determined from that of XRD studies for deposition time below 25 min. are comparable to the Bohr excitonic radius supporting the quantum size effect.

The blue shift of band gap might also be utilized in determining the crystallite radius (r) using relation [16]

$$\Delta E_g = E_{g(\text{film})} - E_{g(\text{bulk})} = [h^2 / 8\mu r^2] - [1.8 e^2 / r \varepsilon] \quad (4)$$

where μ is the reduced mass of electron-hole effective mass and ε is the dielectric constant. From the above equation, the crystallite sizes have been determined and these lie in the range 3.65 nm to 2.82 nm.

The variation of direct band gap and indirect band gap with different deposition times are shown in Fig. 4. It is clear from this figure that both the direct band gap and indirect band gap decreases with increase in deposition time, when the other deposition parameters remain constant. These may be due to stronger quantum confinement at smaller deposition time.

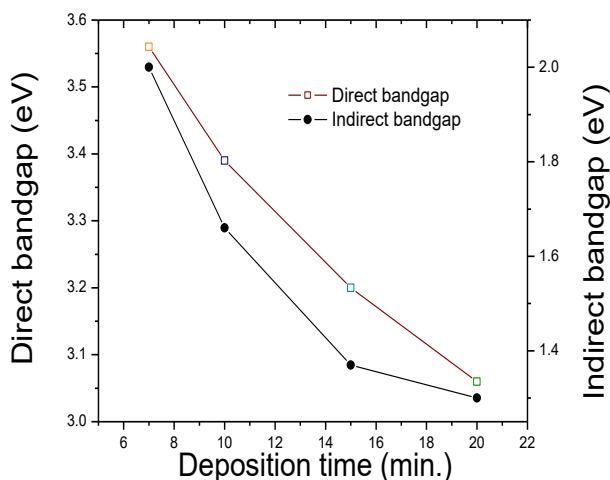


Fig. 4. Variation of direct band gap and indirect band gap of nanocrystalline CdS thin film with deposition time.

The thickness of the films were measured by an ellipsometer and it was in the range 50 nm to 200 nm. for different deposition times. It was also noted that the film thickness increases with the increase of deposition time but the rate of increment gradually decreases with the increase of deposition time.

C. Dielectric property study

Fig. 5 shows the variation of dielectric constant as a function of frequency of the applied a.c. electric field for CdS nanoparticle thin films with different particle size for films deposited with different deposition time such as (a) 10 min., (b) 20 min. and (c) 30 min. The dielectric constant for thin films of CdS nanofibers have been measured under vacuum (10^{-3} mbar) by using an L-C-R meter and the value of it lies in the range 85 to 100 at higher frequencies (as shown in Figure 5) which are much higher than that of bulk CdS having dielectric constant ~ 9 [17]. The large value of dielectric constant of CdS nanofibers thin film is due to the fact that the nanofibers of CdS under the application of electric field, act as nanodipoles. As the size is in nanometer order, the number of crystallites per unit volume is very large; hence the dipole moment per unit volume increases, so the dielectric constant increases. Again, it is clear from the Fig. 5. that the dielectric constant of the films decreases with increase of deposition times. This is due to the fact that with the increase of deposition time, the crystallite size increases, the number of nanocrystallites per unit volume decreases, which implies that under application of electric field, the number of nanodipoles per unit volume decreases.

Hence dielectric constant decreases. It has also been observed that, for each particle size of CdS in the films, the dielectric constant is almost constant at high frequency range i.e. there is no dispersion at high frequency. At higher frequencies the nanodipoles cannot follow the rapid variations of the electric field and hence they show practically no dispersion. Bhattacharya et al [7, 8], also obtained very high dielectric constant without dispersion in their silver nanowires formatted in a polymeric film and in the pores of a silica gel.

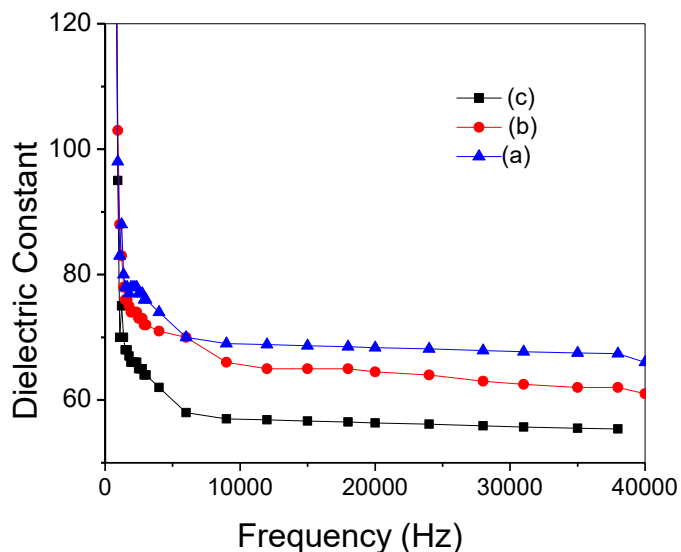


Figure 5 Variation of dielectric constant of nano-CdS thin films with frequency for different deposition time (a) 10 min., (b) 20 min. and (c) 30 min.

The dielectric permittivity of CdS nanofibers is high at lower frequencies. This may be due to the contribution of the electronic, ionic, dipolar and space charge polarizations, which depend on the frequencies (Xue et al and Suresh et al). Space charge polarization is generally active at lower frequencies and indicates the purity and perfection of the nanoparticles [12-13].

In dielectric materials, dielectric losses usually occur due to the absorption current. The orientation of the molecules along the direction of the applied electric field in polar dielectrics requires a part of the electric energy to overcome the forces of internal friction. Another part of the electric energy is utilized for rotations of the dipolar molecules and other kinds of molecular transfer from one position to another, which also involve energy losses.



International Journal of Recent Development in Engineering and Technology

Website: www.ijrdet.com (ISSN 2347-6435(Online) Volume 7, Issue 6, June 2018)

IV. CONCLUSION

CdS nanofibers have been prepared by dc-sputtering technique without using any catalyst. TEM micrograph confirmed the formation of nanofibers with diameter in the range 2 nm to 4.3 nm and length a few microns. XRD studies showed the crystallite size (lie within the range 2.3 nm to 4.6 nm) decreases with decrease in deposition time and the strain (lie in the range 7.2×10^{-2} to 1.95×10^{-2}) increases with the decreases of deposition time. UV-Vis spectra of the films showed the band gap was higher compared to that of the bulk material. The direct optical band gap increased from 3.06 eV to 3.56 eV with decrease of deposition time from 20 to 7 min. The crystallite sizes were also calculated from the shift of direct band gap from that of bulk materials which came out 2.82 nm to 3.65 nm. The dielectric constant for thin films of CdS nanofibers have been measured under vacuum $\sim 10^{-3}$ mbar by using an L-C-R meter and the value of it lies in the range 55 to 73 at higher frequencies.

Acknowledgement

The author wishes to thank Prof. K. K. Chattopadhyay of Thin Film Nanoscience Laboratory, Jadavpur University Kolkata, for all types of supports during the execution of the work.

REFERENCES

- [1] Y. Q. Gao and Y. Bando, Nature 415 (2002) 599.
- [2] J. Bahadur, S. Agrawal, V. Panwar, A. Parveen, K. Pal, Macromolecular Research. (2016) 1–6.
- [3] S. Agrawal, A. Parveen, A. Azam, Mater. Lett. 168 (2016) 125–128.
- [4] S. Agrawal, A. Parveen, A. Azam, J. Magn. Magn. Mater. 414 (2016) 144–152.
- [5] R.K. Duchaniya, Int. J. Mining, Metall. Mech. Eng. 2 (2014) 54–56.
- [6] A. Hasnat and J. Podder Journal Scientific Research, 4 (1), 11-19 (2012)
- [7] Penchal Reddy1*, B.C. Jamalaiah2, I.G. Kim1, D.S. Yoo1, K.V. Siva Kumar3, R. Ramakrishna Reddy, Adv. Mat. Lett. 4(8) (2013) 621-625.
- [8] Salunke Pooja, Jain Preeti, Int. J. Res. Chem. Environ. Vol. 5 (2015) 22-25.
- [9] Sagadevan Suresh, Appl Nanosci 4 (2014) 325–329
- [10] S. Bhattacharya, S. K. Saha, D. Chakravorty, Apl. Phys. Lett. 76 (26) (2000) 3896.
- [11] S. Bhattacharya, S. K. Saha, D. Chakravorty, Apl. Phys. Lett. 77 (23) (2000) 3770.
- [12] Xue D, Kitamura K, Solid State Commun 122 (2002) 537-541.
- [13] Sagadevan Suresh, International Journal of Physical Sciences, Vol. 8(21) (2013)1121-1127.
- [14] J.C.P.D.S. Powder Diffraction File Card 06 - 0314.
- [15] Optical Processes in Semiconductors, Pankove, Prentice-Hall.Inc., 1971.
- [16] A.D. Yoffe, Adv. In Phys. 42 (1993) 173.
- [17] Landolt–Bronstein, Numerical Data and Functional Relationships in Science and Technology, vol. 22a, Springer Verlag, Berlin, 1987, p. 168.